Molecular dynamics simulations of displacement cascades in Fe–10%Cr systems*

Yu Gang(郁 刚)†, Ma Yan(马 雁),
Cai Jun(蔡 军), and Lu Dao-Gang(陆道纲)

School of Nuclear Science and Engineering, North China Electric Power University, Beijing 102206, *China*

(Received 26 November 2010; revised manuscript received 19 August 2011)

Molecular dynamics simulations of the displacement cascades in Fe–10%Cr systems are used to simulate the primary knocked-on atom events of the irradiation damage at temperatures 300, 600, and 750 K with primary knocked-on atom energies between 1 and 15 keV. The results indicate that the vacancies produced by the cascade are all in the central region of the displacement cascade. During the cascade, all recoil Fe and Cr atoms combine with each other to form Fe–Cr or Fe–Fe interstitial dumbbells as well as interstitial clusters. The number and the size of interstitial clusters increase with the energy of the primary knocked-on atom and the temperature. A few large clusters consist of a large number of Fe interstitials with a few Cr atoms, the rest are Fe–Cr clusters with small and medium sizes. The interstitial dumbbells of Fe–Fe and Fe–Cr are in the ⟨111⟩ and ⟨110⟩ series directions, respectively.

Keywords: molecular dynamics simulations, displacement cascades, irradiation damage, primary knocked-on atom

PACS: 61.50.Ah **DOI:** 10.1088/1674-1056/21/3/036101

1. Introduction

High-Cr ferritic/martensitic (F/M) steels are primary candidate structural materials for future nuclear power plants, due to their good void swelling resistance and superior mechanical properties.[1] In future nuclear systems, it is expected that core structural materials will be subjected to severe irradiation and environmental conditions during the reactor's lifetime.[2] Irradiation, in general, leads to the degradation of the mechanical properties of materials, via the creation of radiation defects and secondary phase particles. Both of them hindering the motion and the creation of dislocations in metals and alloys. A quantitative understanding of the mechanisms leading to the change of properties of these steels after long-term exposure to irradiation is therefore recognized to be of high importance for a safe design and operation of innovative nuclear systems.[3]

High-Cr FM steels for nuclear applications, including reduced activation and oxide-dispersed strengthened (ODS) ones, typically contain 7 at.%–14 at.% Cr, while the content of the other alloying elements generally does not exceed 1%–2%. The main alloying element is Cr, and Fe–Cr binary alloys can be used as model materials to study the behaviour of these steels. The degradation of material properties under irradiation is a multi-scale phenomenon, meaning that different physical processes take place at different time and space levels. Nowadays, it is widely accepted that a multi-scale modelling approach provides a practical framework to tackle this problem. This approach begins with the production of atomic-scale defects by individual displacement cascades and ends with plasticity and fracture mechanics treatment of whole components, wherein the response of the material to changes in temperature and/or applied stress is of concern.[4] In this framework, the molecular dynamics (MD) technique is a unique tool used to study the primary damage state due to displacement cascades induced by high energy particles, such as neutrons, ions, and electrons. Over the last decade, MD simulations have been widely used to assess the primary damage state in pure bcc Fe,[5] some Fe-based systems,[6−8] and also Fe–Cr alloys.[9−13] Simulations of displacement cascades in Fe–Cr random alloys have been carried out mostly in Fe–10%Cr alloys,[9−12] and these simulations could be reliably performed only for a Cr concentration ($C_{\rm Cr}$) of 10%, since this was the only concentration that was acceptably described. On

*Project supported by the National Basic Research Program of China (Grant No. 2007CB209803) and the Applied Basic Research Program of Hebei Province, China (Grant No. 10165401P).

†Corresponding author. E-mail: yugang718@gmail.com

© 2012 Chinese Physical Society and IOP Publishing Ltd

the other hand, in alloys with $C_{\rm Cr} < 10\%$, a tendency towards the ordering of Cr atoms is experimentally detected.[14,15] Note that both of these processes take place in the region of temperatures potentially important for technological applications (above 600 K). Moreover, phase transformation can be accelerated under irradiation[16,17] due to self diffusion via radiation-induced defects and, possibly, also to direct in-cascade atomic redistribution.

In this work, we study the primary damage state in Fe–Cr binary alloys with temperature dependence in a region of temperatures above 600 K, addressing the issue of the in-cascade ballistic mixing being sufficient to induce, within the short time frame of the cascade, the redistribution of the Cr atoms as dictated by the acting thermodynamic forces, i.e., the heat of mixing of the corresponding alloy.

In the present MD calculation to 20 ps, the primary damage process and the state of displacement cascades using MD techniques experience ballistic collision in 10^{-6}–0.2 ps, displacement spike formation (local explosion, shock wave, melting to low density droplet) in 0.2–0.3 ps, relaxing (driving out self interstitial atoms (SIAs), atomic mixing and transfer to a super-cooling droplet) in 0.3–3 ps, solidifying and cooling to circumstance temperature in 3–10 ps (forming deleted zone, disorder (or amorphous) region, vacancies-plate collapse, etc.),[18,19] and the following diffusion process in 10–20 ps. Therefore, it is able to address the above-mentioned issues, especially to address the primary damage state at high temperature, which is different from that at low temperature (including the short-term diffusion process at circumstance temperature after completing the whole process of displacement spike).

2. Cascade generation model and analysis method

The cascade generation model and analysis method were used as MD with the MOLDY program.[20] Periodic boundary conditions were imposed on a constant pressure ensemble of atoms with simulation cells containing 0.5 million atoms for the highest energy 15 keV simulations. A Fe–Cr simulation cell with 10% Cr in random body-centre cubic (bcc) lattice positions was created. The interatomic potential used was the PAW version (based on projector augmented wave (PAW) density functional theory results) of the Fe–Cr potential by Olsson *et al.*,[21] which was developed to be used together with the Olsson Cr–Cr potential[21] and the Ackland–Mendelev 2004 Fe–Fe potential.[22] The coefficients of the alloy potential were fitted to the lattice parameter, 0.28553 nm, of Fe90%–Cr10%, a positive heat of mixing for equimolar composition, the binding energy of the mixed ⟨110⟩-dumbbell in bulk Fe, the substitution energy of a Cr atom in bulk Fe, and the mixing enthalpy curve.

At the beginning of the simulation, the particle system was equilibrated for 2 ps at a temperature representative of operating conditions, such as 300, 600, and 750 K (the well-known 475 °C (748 K) embrittlement of high-Cr Fe–Cr alloys due to nano-segregation of chromium). When the lattice was at thermal equilibrium, one atom, the primary knocked-on atom (PKA), was given a momentum corresponding to an energy of 1 keV or so. The time step in the simulation was manually adapted to the PKA velocity, and it could be as low as 10^{-17} s. Once the cascade energy had been mostly dissipated in elastic collisions, a much longer time step was allowed, i.e., 10^{-16}–10^{-15} s. More details on the procedure can be found in Ref. [23].

The cascades were then started by choosing an Fe atom near the centre of the cell as the PKA and giving it a recoil energy, such as 1 keV or so. The direction of the recoil was random. Temperature scaling (with a constant of 100 fs) was adopted in the cell border region (with a thickness of one lattice parameter). The simulation was stopped if the kinetic energy of a border atom was larger than 10 eV, and restarted with the recoil atom placed farther away from the border but keeping the recoil direction the same. The simulation time was 20 ps. The volume was kept constant, and the temperature was scaled at the borders to remove heat from the system.

To analyse the defects a Wigner–Seitz cell, centred at each lattice site, was used. An empty cell corresponded to a vacancy, while two atoms in the same cell have a self-interstitial configuration. We performed a cluster connectivity analysis, which means that a group of defects are interpreted to belong to the same cluster if they are within a given distance from at least one other defect of the same type. This distance is called a (clustering) cut-off radius. The choice of the cut-off radius is governed by the presence of some significant binding energy between alike defects, which is the second nearest neighbour for vacancy defects, and the third nearest neighbour for SIA defects. Special attention was paid to the fraction of

clustered SIAs and vacancies, as well as to the Cr content among SIAs and clustered SIAs.

In order to find the statistical average for the number of surviving Frenkel pairs and defect clusters produced by the cascade with MD simulation, the number of cascades, simulation time and box size (number of atoms) for various temperatures and PKA energy $E_{\rm MD}$ are summarized in Table 1.

Table 1. Summary of number of cascades, simulation time and box size versus temperature and $E_{\rm MD}$.

$E_{\rm MD}$/keV	No. of cascades in Fe–10%Cr			Other parameters	
	300 K	600 K	750 K	Time/ps	Box size
1	10	10	10	20	500094
5	10	10	10	20	500094
10	10	10	10	20	500094
15	10	10	10	20	500094

3. Results and discussion

3.1. Defect number

The average number of surviving Frenkel pairs ($N_{\rm FP}$) for various temperatures at the end of cascade in Fe–10%Cr resulting from the MD simulations is plotted as a function of $E_{\rm MD}$, as shown in Fig. 1(a). The points have been interpolated using the empirical power law, $N_{\rm FP} = AE_{\rm MD}^m$, as proposed by Bacon *et al.*[24] Prefactor A and exponent m obtained in the least-square fit are in agreement with those in previous work on Fe.[25] The exponent increases with temperature increasing from 0.7514 at 300 K to 0.8892 at 750 K. This means that the defect production is more sensitive to PKA energy at 750 K in Fe–10%Cr. Traditionally, the number of Frenkel pairs produced per cascade is estimated using the NRT formula,[26] $N_{\rm NRT} = 0.8E_{\rm D}/2E_{\rm d}$, where $E_{\rm d}$ is the average displacement energy for all crystallographic directions and $E_{\rm D}$ is the fraction of recoil energy that goes into displacement damage, after subtracting the fraction dissipated for electron excitation. Since in the present MD simulations, the interaction between ions and electrons is not included, it is assumed that $E_{\rm D} = E_{\rm MD}$. The defect production efficiency is defined as the ratio of the surviving MD Frenkel pairs to the number of NRT displacements ($N_{\rm FP}/N_{\rm NRT}$). For the sake of comparison, we took $E_{\rm d} = 40$ eV to estimate the number of defects with the NRT formula. The defect production efficiency shown in Fig. 1(b) decreases with the recoil energy to a more or less asymptotic value of about 0.22 for 10 keV at 300 K and 0.20 for 5 keV at 750 K. The asymptotic value of defect production efficiency is not sensitive to temperature above 300 K, but the start point (PKA energy) of asymptotic curve decreases with the operation temperature increasing. These results are similar to those in the pure iron[25] and the asymptotic value of defect production efficiency is reasonable, which is similar and close to the experimental value about the fraction of the number of survive defects in irradiated metals at the normal temperature (about 0.15).[18]

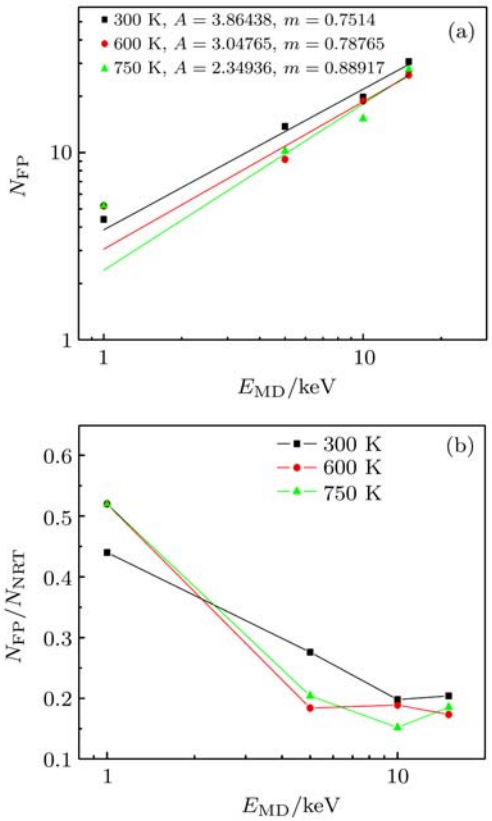


Fig. 1. (colour online) Number of surviving Frenkel pairs (a) and defect production efficiency compared with those from NRT (b) at the end of the cascade versus recoil energy, in Fe–10%Cr with various temperatures. In panel (a), the power law proposed by Bacon *et al.*, $N_{\rm FP} = AE_{\rm MD}^m$, has been used for interpolation.

The present potential predicts a positive binding energy of the mixed ⟨110⟩-dumbbell in bulk Fe. This feature leads to the formation of a number of mixed dumbbells, the fraction of Fe–Cr interstitials in the total number of interstitials is remarkably higher than the fraction of Cr in the matrix at the end of the cascade, as shown in Fig. 2. Above 5 keV of the recoil energy, more than 20% of the final dumbbells contain Cr atoms compared with the 10%Cr concentration of the alloy. Below 5 keV of the recoil energy, the formation of mixed dumbbells increases with the operation temperature. Initially, as expected, more Fe atoms than Cr atoms are displaced and counted as interstitials. However, during the cooling stage, most of these Fe–Fe dumbbells, possibly assisted by the still high temperature, glide till they become trapped at the closest Cr atoms, thereby determining the number of mixed and self-interstitial dumbbells at a higher temperature to be more than that at normal temperature. When the recoil energy is higher than 5 keV, the displacement spike is large enough and the in-cascade ballistic mixing is sufficient to induce, within the short time frame of the cascade, the Cr atom redistribution as dictated by the acting thermodynamic forces, i.e., the heat of mixing of the corresponding alloy, which is of advantage for the formation of Fe–Cr interstitials. In summary, Cr atoms do not appear to significantly affect the collisional stage of the cascade, as may be expected, considering the negligible difference in mass between Fe and Cr atoms. The presence of Cr determines a redistribution of dumbbell species during the post-collisional stage, where the dumbbells is of advantage for containing Cr atoms, in a percentage far higher than the Cr concentration in the alloy, i.e., the fraction of Fe–Cr dumbbells in the total interstitial dumbbells is higher than 10%, produced by the cascade. The direction of Fe–Cr dumbbell is along ⟨110⟩, the same as the direction of Fe–Fe dumbbell along ⟨110⟩, which is in agreement with *ab initio* calculation.[16] The thermal stability of these dumbbells is likely to be responsible for the results in Fig. 2. The fractions of Fe–Cr and Cr–Cr dumbbells in Fe–10%Cr cascades versus recoil energy with various operation temperatures (average evolution of 10 cascades) are shown in Fig. 2, indicating that the ⟨110⟩ Fe–Cr and Cr–Cr dumbbells are more stable than the corresponding defect in pure iron. Consequently, Cr would tend to end up in defect structures forming during the cooling down of recoil cascades.

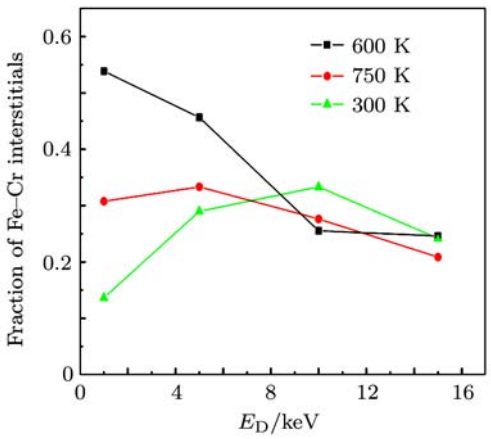


Fig. 2. (colour online) Fractions of the number of Fe–Cr dumbbells interstitials to the number of interstitials versus PKA energy for various temperatures.

3.2. Cluster formation

Previous studies on displacement cascades in Fe show that very little in-cascade vacancy clustering occurs in this material, while sizeable interstitial clusters are found.[11,23–25,27] Our results agree with these findings. The numbers of interstitial clusters versus PKA energy E_D for various temperatures and the size distribution of clusters for E_D as 15 keV at 750 K are shown in Figs. 3(a) and 3(b), which sums the number and the size of interstitial clusters of 10 events for one case, corresponding to 10 cascades with a random emitted direction in one region with time interval 20 ps. The results presented are for a distance between neighbours, 0.49455 nm (the third nearest neighbour). In this calculation, we consider a cluster that contains more than 3 interstitials. The calculation results indicate that the number and the size of interstitial clusters increase with the energy of PKA and is not sensitive to temperature in the range 300–750 K at the PKA energy above 5 keV. Most clusters are less than 8 interstitials in size, but there are always a few larger clusters with some Cr interstitials. The clusters seem to be stabilized by the Fe–Cr mixed interstitial. The Cr fraction distribution in small clusters is shown in Fig. 3(c), showing that the peak of Cr fraction is at 0.25, higher than that in the matrix.

Interstitial clusters can be formed in cascades according to at least three mechanisms. They may be formed when a high-density part, produced during the ballistic phase and lingering on into the nearly melted zone created by the displacement spike, is isolated by a re-crystallisation front.[28] They may also partly form at the end of the displacement spike, as a consequence of collective atomic motion in a condition of enhanced defect diffusion, due to the high

local temperature.[29] Finally, further formation and growth of interstitial clusters may occur by later local defect re-organization, driven by strain-field interaction between neighbouring interstitials and small clusters.[29] While the presence of interstitial-trapping solute atoms can hardly affect the first of these mechanisms, but is expected to greatly influence other two. However, the Fe ⟨111⟩ crowdions and recoils meeting the Cr atom will be "broken" to form the mixed dumbbell, the mixed dumbbell migration will not only enhance the effective stability of mixed dumbbells, but also facilitate the formation of clusters containing a significant number of Cr atoms by the aggregation of single interstitials under the high local temperature of the displacement spike region. Thus there are many small clusters that become stable at the end of a cascade step, which contains Cr as shown in Fig. 3(c).

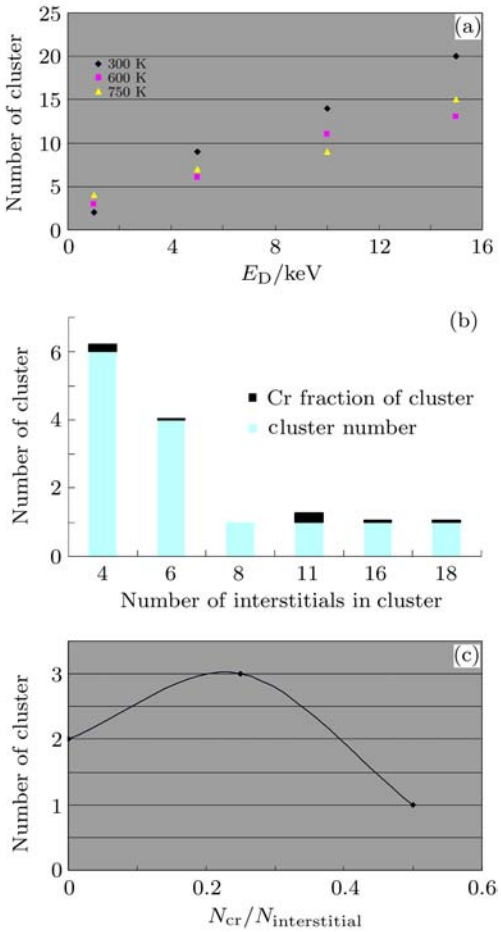


Fig. 3. (colour online) The numbers of interstitial clusters versus PKA energy for 300, 600, and 750 K (a); their size distribution of a cluster in E_D 15 keV at 750 K (b); the number of interstitial clusters versus the fraction of $N_{Cr}/N_{interstitial}$ in a cluster (containing 4 interstitials) for 15 keV at temperature 600 K (c).

At the same time, the large clusters formed in cascades will still be of ⟨111⟩ type Fe crowdions, which can efficiently gather and form clusters, and will still fast glide one-dimensionally toward regions of high Cr concentration, where they will become trapped. Thus, "more interstitials" in clusters means globally "less free" single interstitials suited for being "captured" by Cr atoms and, therefore, less Cr atoms in an interstitial position. Interstitial clusters are formed in cascades in Fe partly at an early stage as a consequence of re-crystallization, partly at the end of the displacement spike as a consequence of collective atomic motion, and partly later, via local defect re-organization, driven by elastic interactions among interstitial defects.

We expect that the formation of Fe–Cr mixed interstitial clusters, which are shown here to be stabilized by Cr, will have a large influence on the subsequent evolution of radiation damage. Because single interstitials in Fe–Cr migrate three-dimensionally, maintaining a ⟨110⟩ dumbbell configuration, with a migration energy of about 0.3 eV. These slowly migrating single ⟨110⟩ dumbbells lead their diffusion into Fe–Cr mixed interstitial clusters, thereby growing, and becoming trapped at Cr atoms and evolving into larger Fe–Cr mixed interstitial clusters. It is due to the fact that three-dimensionally migrating interstitials have, in the long term, more chances of finding a trap than one-dimensionally migrating ones and, in addition, the mixed dumbbells can migrate in a way different from solute-centred crowdions, i.e., once the mixed dumbbell is formed it will not be broken by the process of interstitial migration. This possibility of mixed dumbbell migration will not only enhance the effective stability of mixed dumbbells, but also facilitate the formation of clusters containing a significant number of Cr atoms by the aggregation of single interstitials.

These Fe–Cr mixed interstitial clusters may be obstacles to dislocation motion, leading to the hardening associated with a ductile-brittle transition temperature (DBTT) shift. The observed large number of small sized Fe–Cr mixed interstitial clusters may help explain the experimental observations. A high density of defects with a mean size range in 1.5–6.9 nm was observed, but no cavities, even at the highest studied dose.[30] At operating temperatures higher than 350 °C, the Fe–Cr mixed interstitial clusters will evolve into nanometric dislocation loops with a Burgers' vector $\boldsymbol{b} = a_0\langle 111\rangle/2$ in the {111} plane.

At well-known 475 °C (748 K) the embrittlement of high-Cr Fe–Cr alloy is due to the nano-segregation of chromium. We predict that the ⟨110⟩ Fe–Cr and Cr–Cr dumbbells are more stable than the corresponding defects in pure iron. Consequently, Cr would tend to end up in defect structures forming during the cooling down of recoil cascades.

3.3. Configuration of clusters

The configurations of a 10 keV cascade at 600 K in 10 and 20 ps are shown in Figs. 4(a), 4(b), 4(c) and 4(d). There is no significant difference between them. As we predict, before 10 ps, the cascade experiences ballistic collision (10^{-6}–0.2 ps), a displacement spike process (0.2–3 ps) and solidifying and cooling to circumstance temperature in 3–10 ps. The surviving defects are stable, as shown in Figs. 4(a) and 4(b), then follow the diffusion process in 10–20 ps. The period in 10–20 ps is too short, the surviving defects migrate only slightly and the agglomeration is limited, except the high speed migration of special defects, such as ⟨111⟩ crowdions. Therefore, the configuration of the cascade at 20 ps can be described as the primary damage characterization, and the features of the cascade, such as vacancy spatial distribution, vacancy clusters size and spatial distribution, dumbbell interstitial spatial distribution, interstitial cluster size and spatial distribution, the composition in interstitial cluster, and the interstitial cluster shape (such as nanometer interstitial loops), are taken as a record database for analysis and entering the next code, such as the object kinetic Monte Carlo (OKMC) method[31] for microstructure evolution calculation.

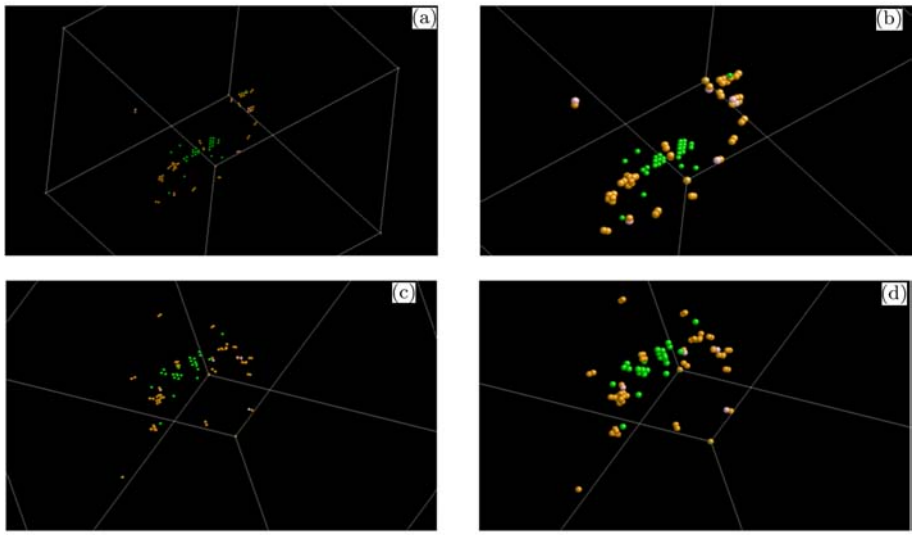


Fig. 4. Configurations of 10 keV cascade in 10 ps (a) zoom-out, (b) zoom-in and 20 ps (c) zoom-out, (d) zoom-in, at 600 K, including spatial distributions of vacancies (green dots) and dumbbell interstitials (yellow dots for Fe, pink dots for Cr), size and spatial distributions of vacancy clusters and interstitial clusters, the composition in interstitial cluster and interstitial cluster shape (such as nanometer interstitial loops), and its spatial clusters.

4. Conclusion

1) The defect production efficiency decreases with recoil energy increasing. The asymptotic value is not sensitive to temperature, but slightly decreases with the operation temperature increasing. It is similar and close to the experimental results for the fraction of the number of surviving defects in irradiated metals at a normal temperature.

2) The interstitials all belong to the ⟨110⟩-dumbbell, the fraction of Fe–Cr mixed interstitials in the interstitials is remarkably higher than that of Cr in the matrix. It indicates that the ⟨110⟩ Fe–Cr and Cr–Cr dumbbells are more stable than the corresponding defect in pure iron.

3) The number and the size of interstitial clusters increase with the energy of the PKA and they are not sensitive to the temperature in a range of 300–750 K.

4) The configurations of 10 keV cascade in 10 and 20 ps indicate that there is no significant difference between them.

Acknowledgements

The authors are grateful to Dr. Robin Schaeublin for the technique guidance and support.

References

[1] Klueh R and Harries D 2001 *High-Chromium Ferritic and Martensitic Steels for Nuclear Applications* (ASTM Intl.) p. 337

[2] Mansur L K, Rowcliffe A F, Nanstad R K, Zinkle S J, Corwin W R and Stoller R E 2004 *J. Nucl. Mater.* **329–333** 166

[3] Zinkle S J 2005 *Phys. Plasmas* **12** 058101

[4] Wirth B D, Caturla M J, de la Rubia T D, Khraishi T and Zbib H 2001 *Nucl. Instrum. and Meth.* B **180** 23

[5] Malerba L 2006 *J. Nucl. Mater.* **351** 28

[6] Calder A F and Bacon D J 1997 *Mater. Res. Soc. Symp.* **439** 521

[7] Calder A F, Bacon D J, Barashev A V and Osetsky Y N 2008 *Philos. Mag. Lett.* **88** 43

[8] Becquart C S, Domain C, van Duysen J C and Raulot J M 2001 *J. Nucl. Mater.* **294** 274

[9] Terentyev D, Malerba L, Chakarova R, Domain C, Nordlund K, Olsson P, Rieth M and Wallenius J 2006 *J. Nucl. Mater.* **349** 119

[10] Björkas C, Nordlund K, Malerba L, Terentyev D and Olsson P 2008 *J. Nucl. Mater.* **372** 312

[11] Malerba L, Terentyev D, Olsson P, Chakarova R and Wallenius J 2004 *J. Nucl. Mater.* **329–333** 1156

[12] Shim J H, Lee H J and Wirth B D 2006 *J. Nucl. Mater.* **351** 56

[13] Wallenius J, Olsson P, Lagerstedt C, Sandberg N, Chakarova R and Pontikis V 2003 *Phys. Rev.* B **69** 094103

[14] Mirebeau I, Hennion M and Parette G 1984 *Phys. Rev. Lett.* **53** 687

[15] Filippova N P, Shabashov V A and Nikolaev A L 2000 *Phys. Met. Metall.* **90** 145

[16] Dubuisson P, Gilbon D and Séran J L 1993 *J. Nucl. Mater.* **205** 178

[17] Mathon M H, de Carlan Y, Geoffroy G, Averty X, Alamo A and de Novion C H 2003 *J. Nucl. Mater.* **312** 236

[18] Yu J 2007 *Radiation Effects on Materials* (Beijing: Chemical Industry Publishing House) (in Chinese)

[19] Björkas C, Nordlund K, Malerba L, Terentyev D and Olsson P 2008 *J. Nucl. Mater.* **372** 312

[20] Finnis M W 1988 *MOLDY6-A Molecular Dynamics Program for Simulation of Pure Metals* (Harwell: AERE R-13182, UKAEA Harwell Laboratory)

[21] Olsson P, Wallenius J, Domain C, Nordlund K and Malerba L 2005 *Phys. Rev.* B **72** 214119

[22] Ackland G J, Mendelev M I, Srolovitz D J, Han S and Barashev A V 2004 *J. Phys.*: *Condens. Matter* **16** S2629

[23] Becquar C S, Domain C, Legris A and van Duysen J C 2000 *J. Nucl. Mater.* **280** 73

[24] Bacon D J, Calder A F and Gao F 1995 *Nucl. Instrum. And Meth.* B **102** 37

[25] Stoller R E 2000 *J. Nucl. Mater.* **276** 22

[26] Norgett M, Robinson M and Torrens I 1975 *Nucl. Eng. Des.* **33** 50

[27] Domain C 2004 *J. Nucl. Mater.* **335** 121

[28] Nordlund K, Ghaly M, Averback R S, Caturla M J, de la Rubia T D and Tarus J 1998 *Phys. Rev.* B **57** 7556

[29] Bacon D J, Calder A F and Gao F 1997 *J. Nucl. Mater.* **251** 1

[30] Schaeublin R and Victoria M 2003 *J. Nucl. Mater.* **283–287** 339

[31] Domain C, Becquart C S and Malerba L 2004 *J. Nucl. Mater.* **335** 121